Title

Energetics of metastudtite and implications for nuclear waste alteration

Journal

Proceedings of the National Academy of Sciences of the United States of America, 111(50)

ISSN

0027-8424

Authors

Guo, Xiaofeng
Ushakov, Sergey V
Labs, Sabrina
et al.

Publication Date

2014-12-16

DOI

10.1073/pnas.1421144111

Peer reviewed

Energetics of metastudtite and implications for nuclear waste alteration

Xiaofeng Guo[a,b], Sergey V. Ushakov[a], Sabrina Labs[c], Hildegard Curtius[c], Dirk Bosbach[c], and Alexandra Navrotsky[a,1]

[a]Peter A. Rock Thermochemistry Laboratory and Nanomaterials in the Environment, Agriculture and Technology Organized Research Unit and [b]Department of Chemistry, University of California, Davis, CA 95616; and [c]Institute of Energy and Climate Research (IEK-6), Nuclear Waste Management, Forschungszentrum Jülich GmbH, 52425 Jülich, Germany

Contributed by Alexandra Navrotsky, November 5, 2014 (sent for review August 28, 2014)

Metastudtite, $(UO_2)O_2(H_2O)_2$, is one of two known natural peroxide minerals, but little is established about its thermodynamic stability. In this work, its standard enthalpy of formation, −1,779.6 ± 1.9 kJ/mol, was obtained by high temperature oxide melt drop solution calorimetry. Decomposition of synthetic metastudtite was characterized by thermogravimetry and differential scanning calorimetry (DSC) with ex situ X-ray diffraction analysis. Four decomposition steps were observed in oxygen atmosphere: water loss around 220 °C associated with an endothermic heat effect accompanied by amorphization; another water loss from 400 °C to 530 °C; oxygen loss from amorphous UO_3 to crystallize orthorhombic α-$UO_{2.9}$; and reduction to crystalline U_3O_8. This detailed characterization allowed calculation of formation enthalpy from heat effects on decomposition measured by DSC and by transposed temperature drop calorimetry, and both these values agree with that from drop solution calorimetry. The data explain the irreversible transformation from studtite to metastudtite, the conditions under which metastudtite may form, and its significant role in the oxidation, corrosion, and dissolution of nuclear fuel in contact with water.

uranium | metastudtite | enthalpy of formation | stability | nuclear fuel alteration

Metastudtite, $(UO_2)O_2(H_2O)_2$, and studtite, $(UO_2)O_2(H_2O)_4$, are the two only known minerals containing peroxide. Metastudtite is the main natural peroxide mineral (1) due to the irreversible dehydration of studtite (2). Both these phases may be found in spent nuclear fuel exposed to water (3–5). Burns et al. (6), by single crystal diffraction of a natural sample, determined the crystal structure of studtite to be monoclinic with space group *C*2/*c*. The structure consists of edge-sharing UO_8-polyhedra chains. The water molecules are located on two different positions between these chains. Although there are different, yet very similar, models for metastudtite, thus far no structure has been determined (7, 8). It is highly probable that metastudtite, like studtite, consists of chains of edge-sharing UO_8 polyhedra with the water molecules located between the chains. To better depict the bonding situation and the different oxygen atoms, it is proposed to write the sum formulas as $(UO_2)(O_2)(H_2O)_2{\cdot}2H_2O$ for studtite and $(UO_2)(O_2)(H_2O)_2$ for metastudtite [in analogy to Burns et al. (6)].

Studtite and other polyoxouranylates have a potentially important role as alteration phases in geological repositories for nuclear waste, specifically regarding the interactions of nuclear waste with the aqueous environment (9, 10). They have also been proposed as corrosion products in sea water after the Fukushima–Daiichi nuclear plant accident (10–12).

In a nuclear waste repository, the high alpha dosage will be the dominant factor after the first thousand years of storage (13). In combination with groundwater, the alpha radiation will lead to formation of H_2O_2 (3, 4, 9, 14). These very localized oxidative conditions could trigger the genesis of studtite or metastudtite even if the overall conditions are reducing (14). The formation of metastudtite on UO_2 samples as a direct effect of alpha radiolysis of water was observed by Sattonay et al. (3). Studtite and metastudtite were identified by Hanson et al. (5) as the only secondary phases left in a 2-y corrosion experiment on spent nuclear fuel. Also $UO_3{\cdot}xH_2O$ ($x < 2$), metaschoepite, was found to form as an oxidation product on the surface of UO_2 samples. On leaching with aqueous H_2O_2 solution, however, it was completely replaced by studtite. The mechanisms by which either phase forms are still unknown. Most safety assessments of nuclear waste repositories regarding the uranium component emphasize the role of the silicates, oxides, and oxyhydroxides. However, Forbes et al. (15) were able to demonstrate that some of these earlier formed phases are susceptible to alteration to studtite.

The decomposition of studtite was first thoroughly studied in 1961 (16–18). Cordfunke and van der Giessen (18) conducted a transmission electron microscopy study of the decomposition in 1963. They found that minor impurities have an influence on the dehydration process, i.e., uranium peroxide synthesized from uranyl nitrate solution behaved differently than uranium peroxide synthesized from uranyl acetate solution during dehydration. Stepwise decomposition of studtite was observed on heating (17, 19). Dehydration of studtite to metastudtite is irreversible (2). Thus far, no mechanism for dehydration has been proposed. The intermediate amorphous phase forming during the first transition (studtite → metastudtite), observed in previous studies (2, 19–24), has not been well investigated. Its identity and following intermediate phases, especially regarding structure, remain unclear. Therefore, decomposition of metastudtite is studied carefully and in depth in this work.

Thermodynamic investigations conducted by Kubatko et al. (14) in 2003 provided the standard enthalpy of formation of studtite to be −2344.7 ± 4.0 kJ/mol. The study also confirmed the stability of studtite, even at low H_2O_2 concentrations in a peroxide-bearing environment, from a thermodynamic point of view. For the first time, to our knowledge, by integrating the differential scanning calorimetry (DSC) trace and using thermogravimetry (TG) results and other thermodynamic data, we were able to

Significance

Uranium peroxides, metastudtite and studtite, can be formed on exposure of UO_2 based nuclear fuels to water during geological disposal or as a result of reactor accidents. We report detailed structural and thermochemical analysis of the metastudtite decomposition process. The thermodynamic data confirm the irreversible transformation from studtite to metastudtite and show that metastudtite can be a major oxidized corrosion product at the surface of UO_2 and contribute a significant pathway to dissolution. The prevalence of metastudtite may require additional tailoring of waste forms to minimize this dissolution pathway for uranium.

Author contributions: X.G., S.V.U., S.L., H.C., D.B., and A.N. designed research; X.G. and S.L. performed research; X.G., S.V.U., S.L., H.C., D.B., and A.N. analyzed data; and X.G., S.V.U., S.L., and A.N. wrote the paper.

The authors declare no conflict of interest.

[1]To whom correspondence should be addressed. Email: anavrotsky@ucdavis.edu.

This article contains supporting information online at www.pnas.org/lookup/suppl/doi:10.1073/pnas.1421144111/-/DCSupplemental.

accurately derive the enthalpy of formation of metastudtite, which was also obtained by high temperature oxide melt solution calorimetric measurements and was found in good agreement with that from the DSC experiment. These data enabled evaluation of its stability in the natural environment.

Results

X-ray diffraction (XRD) patterns shown in Fig. 1*C* were taken on samples covered with kapton foil. This foil protects the samples from air but produces a significant background signal. No additional phases could be observed. Rietveld refinement based on the structure model provided by Weck et al. (8) resulted in the lattice parameters $a = 8.4184(4)$ Å, $b = 8.7671(4)$ Å, and $c = 6.4943(3)$ Å, with wRp = 9.19%, Rp = 7.04%; space group *Pnma*, Z = 4, O3-O3 – distance was constrained. Certain reflection intensities still deviate from the fit. The sample shows strong preferred orientation of the crystallites. Infrared transmission (IR) spectra of metastudtite (Fig. 1*A*) features the typical $\nu(OH)^{asym}$ adsorption band at 3,153 cm^{-1}, which is weaker than in studtite, yet the structures are much sharper. The sharper structures were already observed by Sato (17) in synthetic and by Bastians et al. (25) in natural samples. It is assumed that mainly the crystal water contributes to this signal in the spectrum of studtite. In the Raman spectra (Fig. 1*B*), $\nu(U=O)^{asym}$ is slightly shifted 10 cm^{-1} to higher wave numbers from 921 cm^{-1} in studtite to 933 cm^{-1} in metastudtite. Splitting of this band occurs in the spectrum of metastudtite, which is in accordance with two different U = O bond lengths as proposed by the Weck et al. (8) model. In the Raman spectrum, the symmetric uranyl $\nu(U=O)^{sym}$ stretch appears as the strongest band, followed by the symmetric $\nu(O\text{-}O_{peroxo})$. The region of ~750 cm^{-1}, typical for U-O and (U-O-U-O) long-range modes of UO_3 (26), shows no signal. The presence of amorphous UO_3 in the sample can therefore be excluded.

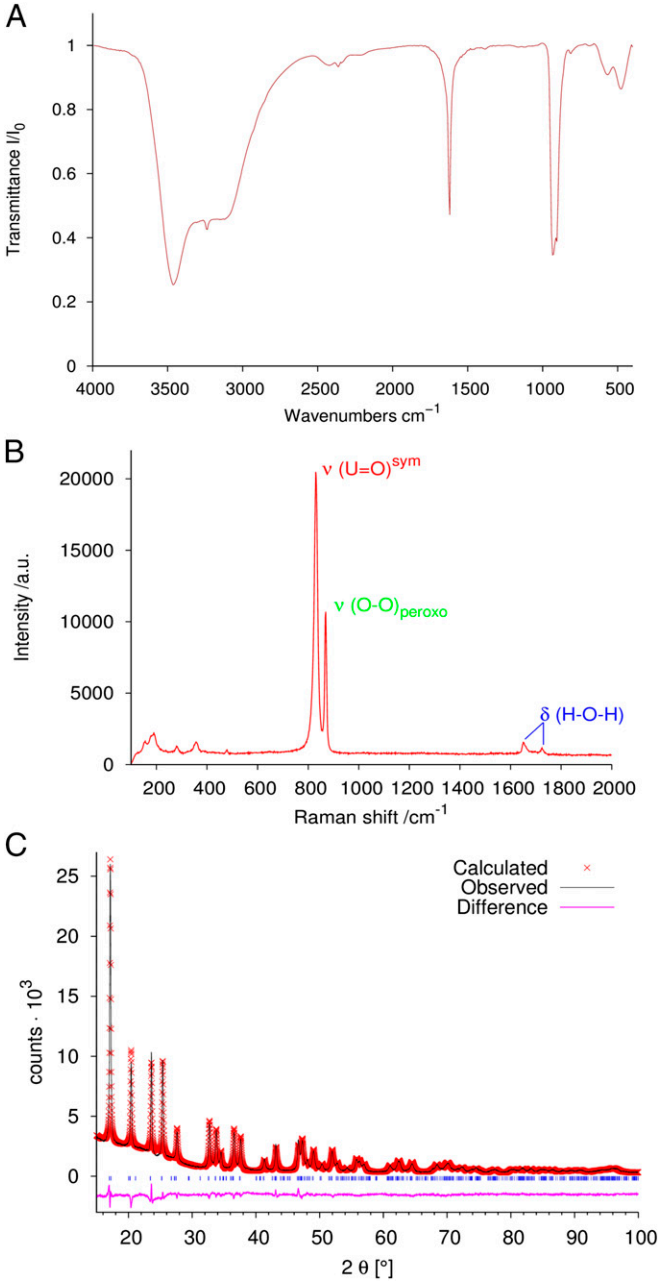

Fig. 1. Metastudtite sample characterization. (*A*) IR spectrum; (*B*) Raman spectrum; and (*C*) Rietveld refinement of XRD pattern of metastudtite (Cu Kα). See text for details.

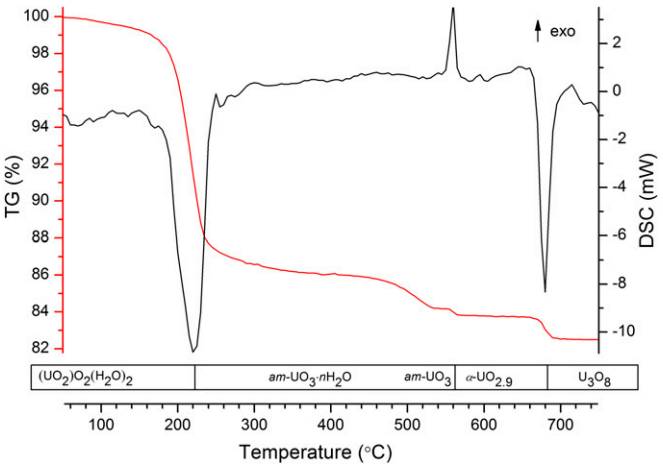

Fig. 2. TG trace in red curve and DSC trace in black curve on metastudtite heating in oxygen.

The DSC trace shows two endothermic and one exothermic heat effects on heating metastudtite to 1,000 °C (Fig. 2). The first endotherm at 180–240 °C is associated with the decomposition of metastudtite to an amorphous phase with evolution of H_2O detected by mass spectrometry. A sample quenched from 300 °C shows no crystalline peaks (Fig. 3), indicating an amorphous phase. This or a similar amorphous phase was identified as different compounds from various studies (2, 19–23). Using both evolved gas and TG analysis (Table 1), we determined it to be amorphous $UO_3{\cdot}nH_2O$ (*am*-$UO_3{\cdot}nH_2O$), which is consistent with previous thermal decomposition experiments (19–21, 23). From 240 °C to 500 °C, TG and DSC indicate loss of water from *am*-$UO_3{\cdot}nH_2O$ to amorphous UO_3 (*am*-UO_3) composition before crystallization, as can be seen in the XRD pattern of sample retrieved at 530 °C (Fig. 3) just before the first exothermic peak. The subsequent exothermic peak reveals the energy released during the crystallization, which is accompanied by loss of oxygen and generating $UO_{2.9}$, an orthorhombic phase (20) that resembles the structure of U_3O_8. The sample retrieved from 580 °C was α-$UO_{2.9}$ (Fig. 3). Continued heating leads to the complete decomposition to U_3O_8, which was identified by XRD on the sample retrieved from 800 °C (Fig. 3). According to DSC analysis, the integrals of first and second endothermic peaks yield 52.3 and 19.9 kJ/mol, respectively, and that of the exothermic peak is –3.5 kJ/mol. Adding these heat effects together gives $\Delta H_{decom} = 68.7$ kJ/mol for the decomposition of metastudtite to U_3O_8 in O_2 atmosphere.

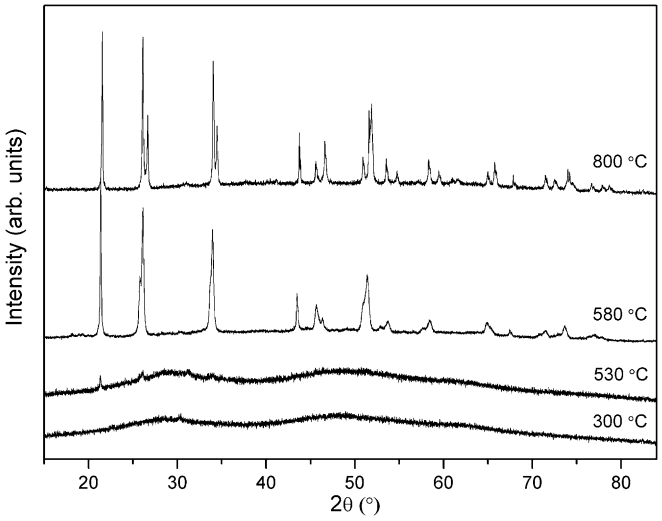

Fig. 3. XRD patterns of metastudtite samples quenched in DSC from indicated temperatures. Pattern above 580 °C corresponds to α-$UO_{2.9}$ (PDF 18–1427) and above 800 °C to U_3O_8 (PDF 61–2801).

Measured drop solution enthalpies from high temperature drop solution calorimetry were used in thermochemical cycles in Table 2 to determine the enthalpy of formation of metastudtite from its oxides. For the reaction

$$\gamma\text{-}UO_{3(s,25\ ^\circ C)} + 2H_2O_{(1,25\ ^\circ C)} + 1/2O_{2(g,25\ ^\circ C)} \rightarrow (UO_2)O_2(H_2O)_{2(s,25\ ^\circ C)}. \quad [1]$$

The enthalpy of formation of metastudtite from γ-UO_3, H_2O, O_2 is determined to be 15.8 ± 1.7 kJ/mol. For analyzing the stability of metastudtite in an environment where H_2O_2 is constantly produced, the following reaction is applied:

$$\gamma\text{-}UO_{3(s,25\ ^\circ C)} + H_2O_{(1,25\ ^\circ C)} + H_2O_{2(1,25\ ^\circ C)} \rightarrow (UO_2)O_2(H_2O)_{2(s,25\ ^\circ C)}. \quad [2]$$

This enthalpy of formation is $\Delta H_{f,ox,peroxide} = -82.3 \pm 1.7$ kJ/mol. Because there are no gases evolved, ΔS is near zero in this reaction; thus, $\Delta G_{f,ox,peroxide}$ is almost equal to $\Delta H_{f,ox,peroxide}$. The negative value indicates that the metastudtite phase is stable with respect to γ-UO_3, H_2O, and neat H_2O_2. In addition, U_3O_8 instead of γ-UO_3 as reference material is valuable for discussion of the long-term stability of metastudtite because U_3O_8 was found to be the final product in both transposed temperature drop (TTD) calorimetry and DSC experiment on decomposition of metastudtite in oxygen. Thus, consider the following reaction based on metastudtite, U_3O_8, H_2O, and O_2

$$1/3\ U_3O_{8(s,25\ ^\circ C)} + 2\ H_2O_{(1,25\ ^\circ C)} + 2/3\ O_{2(g,25\ ^\circ C)} \rightarrow (UO_2)O_2(H_2O)_{2(s,25\ ^\circ C)}. \quad [3]$$

The enthalpy of formation obtained for this reaction is −16.5 ± 2.0 kJ/mol.

Similarly, in the TTD experiment, the final state of metastudtite was well defined (U_3O_8). The thermochemical cycles can thus be easily constructed. Table S1 shows both measured enthalpies and thermochemical cycles associated with the TTD experiment. The enthalpy of formation of metastudtite from U_3O_8, H_2O, and O_2 was therefore obtained to be −12.0 ± 6.8 kJ/mol. This direct measurement agrees, within experimental error, with that done by drop solution calorimetry.

The standard enthalpy of formation, $\Delta H_f^\circ = -1{,}779.6 \pm 1.9$ kJ/mol, was also calculated through thermochemical cycles in Table 2. This result is consistent with data, −1,784.0 ± 4.2 kJ/mol, obtained by combining references (19, 27). All enthalpy of formation results can be found in Table 3.

Discussion

Clearly seen in Fig. 2, the thermal decomposition of metastudtite takes place in different temperature ranges in four steps: (*a*) metastudtite → *am*-$UO_3{\cdot}nH_2O$, (*b*) *am*-$UO_3{\cdot}nH_2O$ → *am*-UO_3, (*c*) *am*-UO_3 → α-$UO_{2.9}$, and (*d*) α-$UO_{2.9}$ → U_3O_8. These steps are elaborated schematically in Fig. 4. Step *a* occurs before 300 °C with an endothermic peak centered at 220 °C, including removal of water and collapse of the peroxide. This decomposition leads to an amorphous phase, which exists around 400 °C (Fig. 4). It is difficult to differentiate this amorphous phase from the *am*-UO_3, which, however, can be easily identified by its composition from TG analysis in Table 1 and its amorphous state from the XRD pattern in Fig. 3. This amorphous form and *am*-UO_3 are bridged by a slow yet noticeable weight loss (removal of water) from 300 °C to 530 °C. Also in this temperature range, the DSC trace suggests that it is loss of water instead of oxygen that leads to the formation of *am*-UO_3, which otherwise would have been observed as obvious and strong DSC signal in that temperature range due to structural change.

Because the compounds formed in those four steps are clear, the weight losses from metastudtite to *am*-$UO_3{\cdot}nH_2O$, *am*-UO_3, α-$UO_{2.9}$, and U_3O_8 are clearly determined and can be compared with their theoretical values (Table 1). The consistency between the experimental and theoretical results is good, with an average difference $\delta^* = 0.35\%$ weight loss for reactions in steps *b*, *c*, and *d*. Thus, $\delta^* = 0.35\%$ as the difference for experimental-theoretical values was applied to the step *a* reaction: metastudtite → *am*-$UO_3{\cdot}nH_2O$. It is then possible to calculate the theoretical value of weight loss of step *a* from subtraction of δ* from experimental value. The chemical composition of product from the step *a* reaction was therefore found to be *am*-$UO_3{\cdot}nH_2O$ ($n = 0.35$), corresponding to the plateau of the TG trace around 400 °C.

Immediately after the second dehydration (step *b* reaction), *am*-UO_3 begins to recrystallize to α-$UO_{2.9}$ with loss of oxygen at 550 °C (step *c* reaction). This crystalline α-$UO_{2.9}$ is identified by

Table 1. TG analysis in O_2 correlating experimental and theoretical weight loss (%)

Step	Experimental weight loss (%)	Theoretical weight loss (%)	Difference δ (%)
$(UO_2)O_2(H_2O)_2$ → *am*-$UO_3{\cdot}nH_2O$	13.90	13.53*	0.35†
$(UO_2)O_2(H_2O)_2$ → *am*-UO_3	15.74	15.39	0.35
$(UO_2)O_2(H_2O)_2$ → $UO_{2.9}$	16.14	15.86	0.28
$(UO_2)O_2(H_2O)_2$ → U_3O_8	17.38	16.70	0.41

Calculated by subtracting δ = 0.35 (and in turn determine the value of *n*).
†Averaging over δ from the following steps.

Table 2. Thermochemical cycles for the calculation of the enthalpies of formation of metastudtite from binary oxides at 25 °C (based on drop solution calorimetry)

Reaction	ΔH (kJ/mol)
(1) $(UO_2)O_2(H_2O)_{2(s,\ 25\ °C)} \rightarrow UO_{3(sln,702\ °C)} + 2\ H_2O_{(g,702\ °C)} + 1/2\ O_{2(g,702\ °C)}$	142.7* ± 0.7†
(2) γ-$UO_{3(s,\ 25\ °C)} \rightarrow UO_{3(sln,\ 702\ °C)}$	9.5 ± 1.5 (28)
(3) $1/3\ U_3O_{8(s,\ 25\ °C)} + 1/6\ O_{2(g,\ 25\ °C)} \rightarrow \gamma$-$UO_{3(s,\ 25\ °C)}$	−32.2 ± 1.1 (29)
(4) $H_2O_{(l,\ 25\ °C)} \rightarrow H_2O_{(g,\ 702\ °C)}$	69.0 (30)
(5) $H_2O_{2(l,\ 25\ °C)} \rightarrow H_2O_{(l,\ 25\ °C)} + 1/2\ O_{2(g,\ 25\ °C)}$	−98.0 (30, 31)
(6) $O_{2(g,\ 25\ °C)} \rightarrow O_{2(g,\ 702\ °C)}$	21.8 (30)
(7) $U_{(s,\ 25\ °C)} + 3/2\ O_{2(g,\ 25\ °C)} \rightarrow \gamma$-$UO_{3(s,\ 25\ °C)}$	−1,223.8 ± 0.8 (29)
(8) $H_{2(g,\ 25\ °C)} + 1/2\ O_{2(g,\ 25\ °C)} \rightarrow H_2O_{(l,\ 25\ °C)}$	−285.8 ± 0.1 (31)
(9) γ-$UO_{3(s,\ 25\ °C)} + 2\ H_2O_{(l,\ 25\ °C)} + 1/2\ O_{2(g,\ 25\ °C)} \rightarrow (UO_2)O_2(H_2O)_{2(s,\ 25\ °C)}$ $\Delta H_{f,ox} = -\Delta H_1 + \Delta H_2 + 2\ \Delta H_4 + 1/2\ \Delta H_6$	15.8 ± 1.7
(10) γ-$UO_{3(s,\ 25\ °C)} + H_2O_{(l,\ 25\ °C)} + H_2O_{2(l,\ 25\ °C)} \rightarrow (UO_2)O_2(H_2O)_{2(s,\ 25\ °C)}$ $\Delta H_{10} = \Delta H_{f,ox,peroxide} = -\Delta H_1 + \Delta H_2 + 2\ \Delta H_4 + \Delta H_5 + 1/2\ \Delta H_6$	−82.3 ± 1.7
(11) $1/3\ U_3O_{8(s,\ 25\ °C)} + 2\ H_2O_{(l,\ 25\ °C)} + 2/3\ O_{2(g,\ 25\ °C)} \rightarrow (UO_2)O_2(H_2O)_{2(s,\ 25\ °C)}$ $\Delta H_{f,ox'} = -\Delta H_1 + \Delta H_2 + \Delta H_3 + 2\ \Delta H_4 + 1/2\ \Delta H_6$	−16.5 ± 2.0
(12) $U_{(s,\ 25\ °C)} + 2\ H_{2(g,\ 25\ °C)} + 3\ O_{2(g,\ 25\ °C)} \rightarrow (UO_2)O_2(H_2O)_{2(s,\ 25\ °C)}$ $\Delta H°_f = \Delta H_9 + \Delta H_7 + 2\Delta H_8$	−1,779.6 ± 1.9

*Average.
†Two SDs of the average value.

the XRD (Fig. 3). TG analysis shows a 0.40% weight loss compared with theoretical loss of 0.47%. Continued heating leads to the final decomposition to U_3O_8 (step *d* reaction), supported both by the TG analysis (Table 1) and by the XRD (Fig. 3) of the retrieved sample.

Thermodynamic data based on the DSC can be used to calculate the formation enthalpy of metastudtite, $\Delta H_{f,ox(DSC)}$, from well-defined reference materials (U_3O_8, H_2O, and O_2) at room temperature. Table S2 shows the DSC integral results, heat content of compounds necessary for calculation, and selected thermochemical cycles, from which the value of $\Delta H_{f,ox(DSC)}$ at room temperature were derived.

However, the heat content of metastudtite at 220 °C (that is essential for conversion of enthalpy of formation of metastudtite from 220 °C to 25 °C) is not readily known. Therefore, we used the enthalpy of the step *a* reaction by the integral of the first peak at 220 °C and heat capacity of *am*-UO_3 (29), H_2O (30), and O_2 (30), to estimate the heat content of metastudtite from 25 °C to 220 °C to be 70.2 ± 4.4 kJ/mol. This result along with the thermochemical cycles for calculation are shown in Table S3. To be noticed, ΔH_f° of metastudtite used for calculation is our derived data, −1,779.6 ± 1.9 kJ/mol, from drop solution calorimetry, which, however, can be replaced by the reference data, −1,784.0 ± 4.2 kJ/mol (19, 27). Based on the thermochemical cycles and data presented (Table S1), $\Delta H_{f,ox(DSC)}$ = −12.6 ± 4.4 kJ/mol was obtained, which is comparable to −16.5 ± 2.0 and −12.0 ± 6.8 kJ/mol, derived from high temperature drop solution and TTD calorimetry, respectively.

Metastudtite has a positive enthalpy of formation ($\Delta H_{f,ox}$ = 15.8 ± 1.7 kJ/mol) with respect to UO_3, O_2, and H_2O (Eq. **1**). Even though the change of entropy is unknown, we can be assured of this value being negative (due to the consumption of O_2 in the reaction that decreases entropy by 205.15 J/mol·K per mole of O_2 reacted) (30). Thus, at ambient temperature, metastudtite is not a stable phase, relative to UO_3, O_2, and H_2O; i.e., UO_3 will not spontaneously oxidize to a peroxide-bearing phase by absorbing oxygen.

On the other hand, compared with U_3O_8, O_2, and H_2O (Eq. **3**), the formation enthalpy ($\Delta H_{f,ox'}$ = −16.5 ± 2.0 kJ/mol) is negative, mainly due to the exothermic oxidation of uranium to be completely hexavalent in metastudtite. However, because of $T\Delta S_{oxygen}$ due to the consumption of O_2, the $T\Delta S$ term at ambient conditions is as negative as −41.4 kJ/mol (30), and the Gibbs free energy of formation of metastudtite, $\Delta G_{f,ox'} = \Delta H_{f,ox'} - T\Delta S_{oxygen}$, is 24.9 ± 2.0 kJ/mol. This positive Gibbs free energy still indicates the unfavorable formation of metastudtite, even as a metastable phase.

The stability of metastudtite is improved under a condition without the consumption of oxygen gas. Previous studies (3, 5, 14) on studtite found its stability was strongly improved when H_2O_2, generated and replenished by radiolysis of water, is present (14). With the presence of H_2O_2, this locally oxidizing condition is also expected to stabilize the metastudtite phase. The formation reaction involving hydrogen peroxide is Eq. **2**. The change of entropy for this reaction should be small because no gas is evolved or consumed. Then the free energy of metastudtite with respect to UO_3, H_2O, and H_2O_2 is mainly dependent on its enthalpy of formation. The strongly negative value of $\Delta H_{f,ox,peroxide}$ = −82.3 ± 1.7 kJ/mol indicates that the formation of metastudtite in presence of hydrogen peroxide and in an oxidizing environment is quite favorable.

Furthermore, both studtite and metastudtite have been suggested to be alteration products of spent nuclear fuel (3, 9, 14). The transformation from studtite to metastudtite or vice versa is important for predicting the long-term products in a geological repository. The reaction from studtite to metastudtite at room temperature is

$$(UO_2)O_2(H_2O)_{4(s,25\ °C)} \rightarrow (UO_2)O_2(H_2O)_{2(s,25\ °C)} + 2H_2O_{(1,25\ °C)}. \quad [4]$$

The enthalpy of reaction was obtained, ΔH_{rxn} = −7.5 ± 3.6 kJ/mol, by using ΔH_{ds} of studtite under the same calorimetric condition,

Table 3. Enthalpies of formation of metastudtite at 25 °C from oxides

Reactants	$\Delta H_{f,ox}$(kJ/mol)[a]	Reference
γ-UO_3, H_2O, and O_2	15.8 ± 1.7	Drop solution calorimetry
γ-UO_3, H_2O, and H_2O_2	−82.3 ± 1.7	Drop solution calorimetry
U_3O_8, H_2O, and O_2	−16.5 ± 2.0	Drop solution calorimetry
	−12.0 ± 6.8	TTD calorimetry
	−12.6 ± 4.4	DSC
	−20.8 ± 4.3	Cordfunke et al. (19, 27)

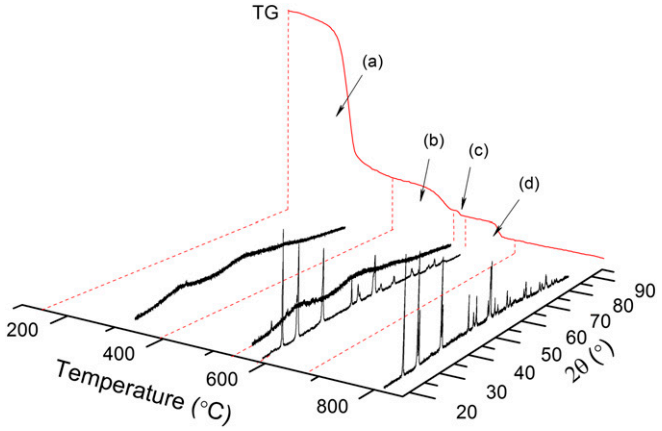

Fig. 4. TG traces on metastudtite heated in oxygen and XRD pattern for each intermediate products from decomposition steps *a* to *d*. Decomposition products were identified from XRD analysis of quenched samples (Fig. 3) and weight loss analysis (Table 1).

273.20 ± 3.6 kJ/mol (14), plus that of metastudtite and water. This exothermic enthalpy of the transformation of a supposed low temperature phase (studtite) to its less hydrous high temperature phase assemblage (metastudtite plus water) confirms that studtite is a metastable phase. Thus, studtite is unlikely to have a thermodynamic stability field and its dehydration to metastudtite is irreversible, as has been generally observed (2, 17, 19–24). The temperature at which studtite is observed to dehydrate is thus controlled by kinetics.

Because the temperature in the repository near field is around 100 °C (3), we can deduce that metastudtite is the most probable phase to persist under repository conditions as long as H_2O_2 continues being produced by radiolysis. Such environmental conditions are found to be crucial in stabilizing peroxide-containing uranyl phases (3, 14). The solubility experiment done by Kubatko et al. (14) on studtite demonstrated the formation of studtite from a solution at 25 °C, pH 3.1, that contains 25 μM of $(UO_2)^{2+}$ and 3.4 mM of H_2O_2. Using $\Delta H_{f,ox,peroxide}$ for both compounds from assemblage (H_2O_2, H_2O, and γ-UO_3), −82.3 ± 1.7 kJ/mol for metastudtite and −75.7 ± 4.1 kJ/mol (14) for studtite, we can estimate in equilibrium concentration of H_2O_2 for forming metastudtite from that of H_2O_2 for studtite based on the following equation: $[H_2O_2]_{metastudtite} \sim e^{(\Delta G(metastudtite) - \Delta G(studtite))/RT} \cdot [H_2O_2]_{studtite}$, where $e^{(\Delta G(metastudtite) - \Delta G(studtite))/RT} = 0.997$. The concentration of H_2O_2 necessary for forming metastudtite is slightly lower than that for studtite. This concentration of H_2O_2 can be easily accumulated in as short as 4 y from radiolysis of water (14), and such alpha particle radiation can be provided by uraninite and its daughter products in U-rich rocks or spent nuclear fuels. Such conditions are rare in natural settings but common at the surface of spent nuclear fuel (14). Thus, metastudtite decomposed from studtite under that condition is also expected based on previous discussion.

The whole pathway of forming metastudtite from spent fuel starts from UO_2 as a main part of spent nuclear fuel, through dissolved uranyl with the presence of aqueous peroxide, to metastudtite as a final product

$$UO_{2(s)} + H_2O_{(l)} + H_2O_{2(l)} + 1/2\ O_{2(g)} \rightarrow (UO_2)O_2(H_2O)_{2(s)}. \quad [5]$$

Using the enthalpy of drop solution (ΔH_{ds}) of UO_2, −136.3 ± 2.3 kJ/mol (32), and those of metastudtite, H_2O, neat H_2O_2, and O_2, we obtained the enthalpy of reaction from UO_2 to metastudtite: −217.1 ± 2.4 kJ/mol. The corrosion (Eq. **5**) was found to be energetically favorable. Taking into account the lower concentration of peroxide in solution and the various entropy terms in the reaction will make the free energy of reaction less negative than the enthalpy above but is unlikely to change its sign. The thermodynamic analysis above supports the conclusion that uranyl peroxide phases are important in spent fuel corrosion. Once they are formed, they can decompose to soluble species (including both dissolved uranyl species and uranyl peroxide clusters) (10), providing pathways for the transport of uranium away from the corroding fuel surface and regenerating additional fresh surface for continuing corrosion.

Conclusions

We studied the thermal behavior of metastudtite in oxygen from room temperature to 1,000 °C, observed stepwise decomposition of metastudtite, and reported reaction enthalpies corresponding to each stage of decomposition. Through carefully using those DSC data and other thermodynamic data from references, we are able to estimate the enthalpy of formation of metastudtite with good accuracy. High temperature oxide melt solution calorimetry yielded an enthalpy of formation consistent with TTD calorimetry- and DSC-derived results. These thermodynamic data further indicate the irreversibility of the transformation of studtite to metastudtite. Metastudtite is stable and persistent in the presence of hydrogen peroxide generated by water radiolysis at the surface of spent nuclear fuel in storage or in a repository.

Materials and Methods

All reagents, unless otherwise mentioned, were analytical grade and obtained from Merck KGaA Darmstadt. Studtite was synthesized from an acidic (HCl, pH ~ 3) aqueous UO_2 suspension by slowly adding a 30% (wt/wt) H_2O_2 solution to the mixture. The H_2O_2 solution is added one drop per minute. After the desired amount has been added, the mixture was stirred for an additional 24 h at room temperature. The obtained light yellow precipitate was filtered, washed with demineralized water, and then dried at ambient temperature. Finally, metastudtite was obtained by dehydrating the prepared studtite at 90 °C for 48 h. Synthesis and initial characterization were performed in Jülich, Germany, after which the sample was shipped to University of California, Davis for calorimetry.

XRD measurements were performed with Bruker D4 and D8 diffractometers with Bragg-Brentano geometry (Cu $K\alpha_{1/2}$ radiation, $\lambda_1 = 1.5056$ Å, $\lambda_2 = 1.54441$ Å, 40 kV, 40 mA), equipped with a LynxEye linear position-sensitive detector and fixed divergence slit, a step size of 0.022°, with an exposure time of 1 s in the range $2\theta = 10$–$130°$.

IR measurements were performed with a Bruker Equinox 55 TGA-IR instrument using a sample embedded in a KBr pellet. Raman spectra was taken with a Renishaw Raman spectrometer (RM-100) equipped with a Leica DMLM optical microscope with a grating with 1,800 grooves/mm and a Peltier-cooled charge-coupled device (CCD). For excitation, the λ = 532-nm line of a Nd:YAG laser with a maximum power of 20 mW was used.

Thermal analysis to 1,000 °C was performed with a Netzsch 449 TG/DSC in O_2 flow 40 mL/min with 10 °C/min heating rate using samples 14.5 mg in weight. The sensitivity was calibrated by the heat capacity method with an Al_2O_3 standard. Gases evolved on sample decomposition were analyzed with the quadrupole mass spectrometer MKS Cirrus 2. For unambiguous identification of phase transformations observed with thermal analysis, multiple experiments were performed to different temperatures followed by XRD analysis of recovered samples.

A custom-built Tian-Calvet twin microcalorimeter (33, 34) operated at 702 °C was used for measurements of ΔH_{ds} of metastudtite in molten sodium molybdate ($3NaO{\cdot}4MoO_3$) solvent and for TTD calorimetry in empty platinum crucibles. For drop experiments, metastudtite powder was hand pressed in pellets ~5 mg in weight and weighed on a microbalance. The sample chamber was flushed with O_2 at ~50 mL/min. In drop solution experiments, O_2 was also bubbled through the melt to maintain oxidizing condition and facilitate dissolution of samples by preventing local saturation (35). The calorimeter was calibrated by transposed temperature drop of ~5 mg Al_2O_3 against its heat content (33, 34). Four drop solution experiments and five transposed temperature drop experiments were performed to evaluate reproducibility of measurements. Uncertainties are reported as 2 SDs of the mean. The equipment, calibration, and experimental method have been described in detail elsewhere (33, 34).

To calculate enthalpies of formation from drop calorimetry experiments, the final state of the dropped sample must be known. The dissolution of metastudtite sample in molten $3NaO{\cdot}4MoO_3$ solvent was confirmed by a

furnace test conducted at 700 °C, where ~5 mg of sample was dropped into molten $3NaO{\cdot}4MoO_3$, and a clear solution was observed after ~25 min. The ready and complete dissolution of U(VI) compounds in molten $3NaO{\cdot}4MoO_3$ was described previously and hexavalent U in dilute solution in sodium molybdate melt was confirmed (32). Samples after the TTD calorimetry experiment were retrieved and analyzed by XRD, and the product of decomposition was identified as U_3O_8.

ACKNOWLEDGMENTS. Metastudtite synthesis and part of the characterization were done at Forschungszentrum Jülich, Germany. We thank Dr. J. D. Bauer for collection of the Raman spectra. The calorimetric work data analysis, paper writing, and personnel support (X.G., S.V.U., and A.N.) at University of California, Davis were supported as part of the Materials Science of Actinides, an Energy Frontier Research Center funded by the US Department of Energy, Office of Science, Office of Basic Energy Sciences under Award DESC0001089.

1. Deliens M, Piret P (1983) Metastudtite, $UO_4{\cdot}2H_2O$, a new mineral from Shinkolobwe, Shaba, Zaire. *Amer Miner* 68(3-4):456–458.
2. Walenta K (1974) Studtite and its composition. *Am Miner* 59(1-2):166–171.
3. Sattonnay G, et al. (2001) Alpha-radiolysis effects on UO_2 alteration in water. *J Nucl Mater* 288(1):11–19.
4. Amme M (2002) Contrary effects of the water radiolysis product H_2O_2 upon the dissolution of nuclear fuel in natural ground water and deionized water. *Radiochim Acta* 90(7):399–406.
5. Hanson B, et al. (2005) Corrosion of commercial spent nuclear fuel. 1. Formation of studtite and metastudtite. *Radiochim Acta* 93(3):159–168.
6. Burns PC, Hughes K-A (2003) Studtite, $[(UO_2)(O_2)(H_2O)_2](H_2O)_2$: The first structure of a peroxide mineral. *Am Miner* 88(7):1165–1168.
7. Ostanin S, Zeller P (2007) Ab initio study of uranyl peroxides: Electronic factors behind the phase stability. *Phys Rev B* 75(7):073101–073104.
8. Weck PF, Kim E, Jové-Colón CF, Sassani DC (2012) Structures of uranyl peroxide hydrates: A first-principles study of studtite and metastudtite. *Dalton Trans* 41(32): 9748–9752.
9. McNamara B, Buck E, Hanson B (2002) Observation of studtite and metastudtite on spent fuel. *Mater Res Soc Symp P* 757:401–406.
10. Armstrong CR, et al. (2012) Uranyl peroxide enhanced nuclear fuel corrosion in seawater. *Proc Natl Acad Sci USA* 109(6):1874–1877.
11. Burakov BE, Strykanova EE, Anderson EB (1997) Secondary uranium minerals on the surface of Chernobyl ''lava''. *Mat Res S C* 465:1309–1311.
12. Burns PC, Ewing RC, Navrotsky A (2012) Nuclear fuel in a reactor accident. *Science* 335(6073):1184–1188.
13. Bodansky D (1996) *Nuclear Energy: Principles, Practices, and Prospects* (American Institute of Physics, Woodbury, NY), pp 246–273.
14. Kubatko K-AH, Helean KB, Navrotsky A, Burns PC (2003) Stability of peroxide-containing uranyl minerals. *Science* 302(5648):1191–1193.
15. Forbes TZ, Horan P, Devine T, McInnis D, Burns PC (2011) Alteration of dehydrated schoepite and soddyite to studtite, $[(UO_2)(O_2)(H_2O)_2](H_2O)_2$. *Am Miner* 96(1):202–206.
16. Ukazi R (1959) On the reactivity of uranouranic oxide, (I) On the thermal decomposition of uranyl nitrate (UNH), ammonium diuranate (ADU) and uranium peroxide (UPO). *J Atomic Energy Soc Japan* 1(7):405–411.
17. Sato T (1961) Thermal decomposition of uranium peroxide hydrate. *Naturwissenschaften* 48(22):693.
18. Cordfunke EHP, Vandergiessen AA (1963) Pseudomorphic decomposition of uranium peroxide into UO_3. *J Inorg Nucl Chem* 25(5):553–555.
19. Cordfunke EHP, Aling P (1963) Thermal decomposition of hydrated uranium peroxides. *Recl Trav Chim Pays Bas* 82(3):257–263.
20. Wheeler VJ, Dell RM, Wait E (1964) Uranium trioxide and the UO_3 hydrates. *J Inorg Nucl Chem* 26(11):1829–1845.
21. Rocchicc C (1966) Etude par thermogravimetrie analyse thermique differentielle et spectrographie dabsorption infrarouge des hydrates du peroxyde duranium. *Cr Acad Sci B Phys* 263(19):1061–1063.
22. Sato T (1976) Thermal-decomposition of uranium peroxide hydrates. *J Appl Chem Biotechn* 26(4):207–213.
23. Cejka J, Sejkora J, Deliens M (1996) New data on studtite, $UO_4{\cdot}4H_2O$, from Shinkolobwe, Shaba, Zaire. *Neues Jb Miner Monat* 3(3):125–134.
24. Rey A, Casas I, Gimenez J, Quinones J, de Pablo J (2009) Effect of temperature on studtite stability: Thermogravimetry and differential scanning calorimetry investigations. *J Nucl Mater* 385(2):467–473.
25. Bastians S, Crump G, Griffith WP, Withnall R (2004) Raspite and studtite: Raman spectra of two unique minerals. *J Raman Spectrosc* 35(8-9):726–731.
26. Lipp MJ, Jenei Z, Park-Klepeis J, Evans WJ (2011) *Raman Investigation of the Uranium Compounds U_3O_8, UF_4, UH_3 and UO_3 Under Pressure at Room Temperature* (Lawrence Livermore National Laboratory, Livermore, CA).
27. Cordfunke EHP (1966) *Thermodynamic Properties of Hexavalent Uranium Compounds* (International Atomic Energy Agency, Vienna), Vol 2, pp 483–495.
28. Helean KB, et al. (2002) Enthalpies of formation of Ce-pyrochlore, $Ca_{0.93}Ce_{1.00}Ti_{2.035}O_{7.00}$, U-pyrochlore, $Ca_{1.46}U^{4+}{}_{0.23}U^{6+}{}_{0.46}Ti_{1.85}O_{7.00}$ and Gd-pyrochlore, $Gd_2Ti_2O_7$: Three materials relevant to the proposed waste form for excess weapons plutonium. *J Nucl Mater* 303(2-3):226–239.
29. Grenthe I, et al. (1992) *Chemical Thermodynamics of Uranium* (Elsevier, Amsterdam), p 31, 61.
30. Chase MW, Jr (1998) NIST-JANAF Thermochemical Tables, Fourth Edition. *J Phys Chem Ref Data, Monograph* 9:1–1951.
31. Robie RA, Hemingway BS (1995) Thermodynamic properties of minerals and related substances at 298.15 K and 1 bar pressure and at higher temperatures. *US Geol Surv Bull* 2131:16.
32. Helean KB, et al. (2003) Enthalpies of formation of U-, Th-, Ce-brannerite: Implications for plutonium immobilization. *J Nucl Mater* 320(3):231–244.
33. Navrotsky A (1977) Progress and new directions in high-temperature calorimetry. *Phys Chem Miner* 2(1-2):89–104.
34. Navrotsky A (1997) Progress and new directions in high temperature calorimetry revisited. *Phys Chem Miner* 24(3):222–241.
35. Navrotsky A, et al. (1994) The behavior of H_2O and CO_2 in high-temperature lead borate solution calorimetry of volatile-bearing phases. *Amer Miner* 79(11-12): 1099–1109.